Energy transport in a disordered spin chain with broken U(1) symmetry: Diffusion, subdiffusion, and many-body localization

M. Schulz, S. R. Taylor, C. A. Hooley, and A. Scardicchio

Phys. Rev. B **98**, 180201 — Published 5 November 2018

DOI: 10.1103/PhysRevB.98.180201

Energy transport in a disordered spin chain with broken U(1) symmetry: diffusion, subdiffusion, and many-body localization

M. Schulz*,[1,2] S.R. Taylor*,[1] C.A. Hooley,[1] and A. Scardicchio[3,4]

[1] *SUPA, School of Physics and Astronomy, University of St Andrews, North Haugh, St Andrews, Fife KY16 9SS, United Kingdom*

[2] *Max Planck Institute for the Physics of Complex Systems, Nöthnitzer Str. 38, 01187 Dresden, Germany*

[3] *The Abdus Salam International Center for Theoretical Physics, Strada Costiera 11, 34151 Trieste, Italy*

[4] *INFN Sezione di Trieste, Via Valerio 2, 34127 Trieste, Italy*

(Dated: Wednesday 23rd May 2018)

We explore the physics of the disordered XYZ spin chain using two complementary numerical techniques: exact diagonalization (ED) on chains of up to 17 spins, and time-evolving block decimation (TEBD) on chains of up to 400 spins. Our principal findings are as follows. First, we verify that the clean XYZ spin chain shows ballistic energy transport for all parameter values that we investigated. Second, for weak disorder there is a stable diffusive region that persists up to a critical disorder strength that depends on the XY anisotropy. Third, for disorder strengths above this critical value energy transport becomes increasingly subdiffusive. Fourth, the many-body localization transition moves to significantly higher disorder strengths as the XY anisotropy is increased. We discuss these results, and their relation to our current physical picture of subdiffusion in the approach to many-body localization.

PACS numbers: 75.10.Pq, 71.23.An, 66.30.Xj

Introduction. Although quantum mechanics is over a hundred years old, some of its most striking predictions about macroscopic systems have been overlooked until recently. Now, however, technological progress in isolating and controlling nano- and mesoscopic quantum systems [1, 2] has led to renewed interest in their fundamental properties. These newly available experimental avenues, and the associated computational and analytical progress, are once again bringing questions about the quantum mechanics of macroscopic systems to the fore.

One recent prediction is the typicality of a localized phase in strongly disordered quantum systems, an effect known as many-body localization (MBL) [3–7]. For non-interacting systems, it has long been known from the work of Anderson [8] (and the large amount of numerical and analytical work that followed [9]) that, when the disorder is sufficiently strong, transport stops. Examples include impurity-band electrons in a semiconductor at sufficiently low densities [10] and waves propagating in a medium with an irregular dielectric constant [11].

Recent works aimed at determining what localization means for interacting systems have shown the phenomenology of these 'transportless' MBL systems to be quite rich. Their novel physics includes the slow but continued growth of entanglement measures due to dephasing [12–16] and the emergence of integrability [17–20]. The latter has important implications for future technologies, in particular for quantum computation [21–23].

While there are ongoing debates about the differences between one-dimensional chains and higher-dimensional lattices [24–26], and about the existence or non-existence of a transition in energy at fixed disorder strength [27–29], the basic physics of the MBL phase is nonetheless fairly well understood by now. By contrast, very little progress has been made on the properties of the transition between the ergodic and MBL phases, and in particular the region immediately preceding it on the low-disorder side. Numerics in the critical and pre-critical regions of the isolated system scarcely converge, and the critical exponents that emerge from a scaling analysis appear to be ruled out by general considerations [27, 30, 31].

It is thus useful to observe that one can access much larger system sizes by considering open-system dynamics. Previous papers have pursued this idea to characterize transport in XXZ spin chains, where the z-projection of the total spin is conserved: spin transport in [32–34], and energy transport in [35] though with severely limited numerics. To summarize the results of [32], there is a small region of diffusive transport and a large, pre-critical region of subdiffusive transport.

In this paper we investigate the physics of the disordered spin-1/2 XYZ chain. We choose this model because it is a quantum spin chain in which all conservation laws are violated except energy. In particular, the U(1) symmetry of the XXZ model, which corresponds in a fermionic picture to fermion number conservation, is broken in the XYZ model. Our investigation employs two complementary techniques. First, we time-evolve open chains of up to 400 spins using time-evolving block decimation (TEBD). This method, shown schematically in Fig. 1(a), gives us access to the transport properties of the system at weak-to-intermediate disorder strengths, including the subdiffusive region. Second, we use exact diagonalization (ED) on chains of up to 17 spins, which gives us access to the spectral properties of the system at strong disorder, including the MBL transition itself.

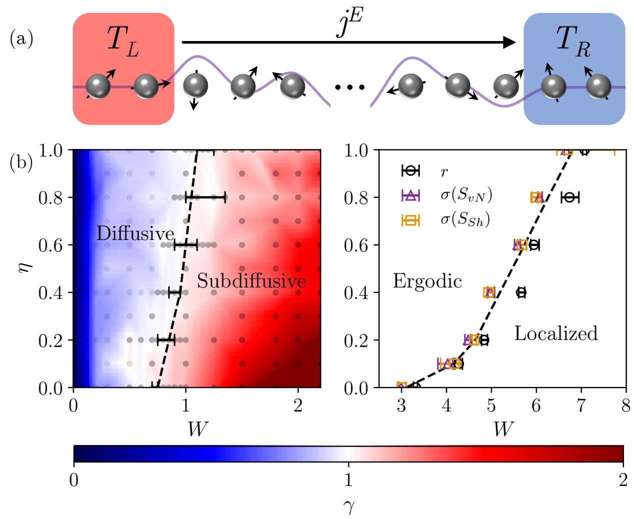

FIG. 1. (a) A disordered spin-1/2 XYZ chain, with Lindblad driving applied to the pair of spins at each end to impose a temperature gradient. In our time-evolving block decimation (TEBD) studies, we time-evolve such a system until it reaches its non-equilibrium steady state (NESS). We supplement that analysis by exact diagonalization (ED) studies on closed (and much shorter) chains. (b) The resulting 'phase diagram' of the disordered spin-1/2 XYZ chain, for an Ising anisotropy of $\Delta = 1.2$. Here η is the XY anisotropy of the exchange interaction between the spins, and W is the strength of the random-field disorder. In the left-hand panel, the dashed line shows the border between diffusive and subdiffusive energy transport determined from our TEBD studies, and the bars are error estimates. The color scale shows the transport exponent γ estimated via interpolation between the numerically determined values, which are indicated by gray points. The right-hand panel shows the location of the MBL transition, determined by three different analyses of our ED results: the crossover in level statistics from random-matrix to Poissonian, r; the peak in the standard deviation of the Shannon entropy, $\sigma(S_{\rm Sh})$; and the peak in the standard deviation of the von Neumann entropy, $\sigma(S_{\rm vN})$.

Summary of main results. Our principal findings are as follows:

First, we verify that in the absence of disorder ($W = 0$) the transport is ballistic [36], in contrast with the classical model [37] where the non-linear interaction between the spin modes causes spin waves to diffuse. We attribute this behavior to the integrability of the quantum model [38], as non-integrable or classical spin chains typically show diffusive transport (see for example [39–41]).

Second, for weak but non-zero disorder ($0 < W \lesssim 0.7$) there is a region in which energy transport is diffusive. This diffusive region persists up to a finite critical disorder strength, $W_{c1}(\eta)$, which depends on the XY anisotropy η (i.e. on how strongly the U(1) symmetry of the XXZ chain is broken).

Third, for increasing disorder strengths $W > W_{c1}(\eta)$ energy transport becomes increasingly subdiffusive, while increasing the XY anisotropy η counteracts this effect and brings the system back towards the regime of diffusive energy transport. We can follow this behavior up to disorder strengths of $W \approx 2.2$, where we see subdiffusive exponents up to $\gamma \approx 2.7$.

Fourth, the system exhibits an MBL transition at a disorder strength $W_{c2}(\eta)$, which increases significantly as the XY anisotropy η is increased. Due to the above-mentioned lack of a U(1) symmetry in the XYZ chain, this transition cannot be thought of as directly following from the arguments for localization of [3]. It is, however, in line with the most recent research on the topic which relies less on the particle interpretation [42] and more on non-proliferation of resonances. We determine W_{c2} via ED analysis of chains with lengths up to $L = 17$ spins, using the standard tests of the eigenstates and spectrum of the Hamiltonian [4, 27, 43, 44].

A phase diagram summarizing these results is shown in Fig. 1(b). In the remainder of this paper we present the details of the model under study and the methods we use, and then proceed to discuss each of these results in turn.

Model. The Hamiltonian of the disordered XYZ spin chain is

$$H = \sum_{n=1}^{L-1} \Big[(1+\eta) s_n^x s_{n+1}^x + (1-\eta) s_n^y s_{n+1}^y + \Delta s_n^z s_{n+1}^z \Big] + \sum_{n=1}^{L} h_n s_n^z. \quad (1)$$

Here $s_n^\alpha = \frac{1}{2}\sigma_n^\alpha$ are spin-1/2 operators (σ_n^α are Pauli matrices), η is the XY anisotropy of the coupling (the parameter that breaks the U(1) symmetry of the XXZ model), Δ is the Ising anisotropy, and $h_n \in [-W, W]$ are uncorrelated disorder fields randomly drawn from a uniform distribution. The $\eta \to 0$ limit of this model is the well-studied XXZ spin chain; $\eta \neq 0$ introduces a term equal to $\eta \sum_n \left(s_n^+ s_{n+1}^+ + s_n^- s_{n+1}^- \right)/2$, which violates the conservation of the z-component of the total magnetization. In the fermion language this corresponds to a nearest-neighbor pairing term.

Methods. We use two complementary methods: TEBD on open chains, and ED on closed ones. In our TEBD studies we couple the ends of the chain to two thermal baths at different temperatures, and describe the time-evolution of the resulting open system using the Lindblad equation [45]

$$\frac{d\rho}{dt} = -i\,[H,\rho] + \kappa \left\{ \mathcal{L}_L(\rho) + \mathcal{L}_R(\rho) \right\}. \quad (2)$$

The first term on the right-hand side of (2) describes the coherent dynamics; the Lindblad terms $\mathcal{L}_L(\rho)$ and $\mathcal{L}_R(\rho)$ correspond to the left and right reservoirs respectively, and κ is the strength with which we couple them to the chain. We apply a two-site thermal driving protocol that

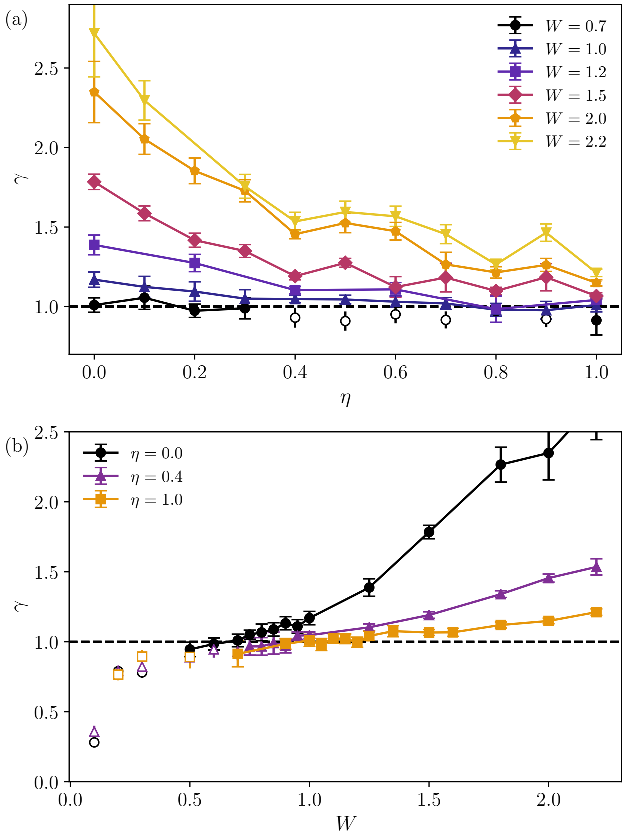

FIG. 2. The energy-transport exponent γ in the disordered spin-1/2 XYZ chain at weak to moderate disorder strengths, as determined from our TEBD numerical results. All results reported are for an Ising anisotropy of $\Delta = 1.2$. (a) The exponent γ as a function of the XY anisotropy η, for various values of the disorder strength W. $\gamma = 1$ corresponds to diffusive energy transport; for $\gamma > 1$, energy transport is subdiffusive. (b) The exponent γ as a function of the disorder strength W, for various values of the XY anisotropy η. The open symbols in both panels indicate cases in which the chain was not long enough to achieve fully diffusive behavior, and these points should therefore be disregarded (see Fig. 3 and corresponding text).

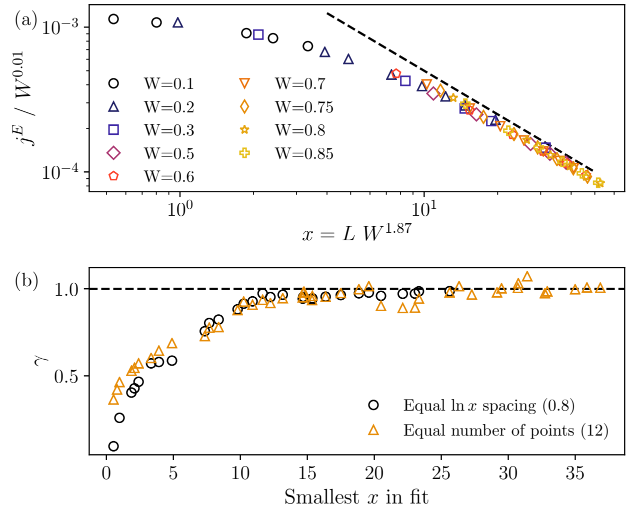

FIG. 3. Testing whether our chains are long enough for the scaling limit to have been reached. In this example the XY anisotropy parameter $\eta = 0.4$. (a) The numerical collapse of the energy current j^E as a function of chain length L onto a single curve under suitable scaling by the disorder strength W. Note the typical crossover from ballistic behavior in short chains to diffusive behavior — indicated by the dashed line — in longer ones. (b) The 'running exponent' $\gamma(x)$, determined from tangential power-law fits to the universal curve, showing that γ reaches the diffusive value of 1 above the critical length scale $x^\star \approx 25 - 30$.

has been used in similar transport studies [46, 47], which drives an isolated pair of spins to a thermal state with temperature T, $\rho \propto \exp(-H/T)$. We drive the pair of spins on the left-hand end of the chain towards a high temperature T_L, and the right-hand pair towards a lower temperature T_R, as depicted in Fig. 1(a). For the remainder of this paper we use the target temperatures $T_L = \infty$ and $T_R = 20$.

We then solve (2) via TEBD to find the nonequilibrium steady state (NESS) energy current in the chain, j^E, for various values of its length, L. The TEBD approach permits us to reach very large system sizes of up to $L = 400$ spins, avoiding the severe finite-size effects described in [32]. Details of our simulation can be found in the Supplemental Material [48]. We then analyze the scaling of $j^E(L)$ with the length of the system L. In the delocalized region preceding the MBL transition we expect the current to scale as $j^E \sim L^{-\gamma}$, where $\gamma = 0$ corresponds to ballistic transport, $\gamma = 1$ to diffusion, and $\gamma > 1$ to anomalous subdiffusive transport [32]. The results of this analysis are shown in Fig. 2.

Because the convergence of our TEBD method worsens at stronger disorder, we cannot use it all the way to the MBL transition. Therefore, we also perform ED studies on short, closed chains (up to $L = 17$ spins for the XXZ model and $L = 16$ spins for the XYZ model) with periodic boundary conditions. We identify the location of the MBL transition using the crossover from random-matrix to Poissonian statistics in the eigenenergy spectrum and the peaks in the fluctuations of the Shannon entropy S_{Sh} and the half-chain entanglement entropy S_{vN}. We evaluate these quantities using the 200 eigenstates closest to the middle of the many-body energy spectrum, and then average over disorder realizations. We then determine the location of the MBL transition by performing a finite-size scaling analysis of the disorder-averaged results. The results of this analysis are shown in Fig. 4.

No disorder: ballistic energy transport. In the limit of no disorder ($W = 0$), we find that the energy current

j^E is independent of the length of the system, which signals that the energy transport is ballistic; this is consistent with previous work on the XYZ model [36]. Ballistic energy transport has been linked to the integrability of quantum systems [49], a characteristic which is also visible in the Poissonian statistics of the Hamiltonian's eigenenergy spectrum [50]. For $0 < \Delta \leq 2$ and $0 < \eta \leq 1$ we find that the average of r falls close to the Poissonian value $r_P = \ln 4 - 1$ over the entire spectrum. Details of this analysis can be found in the Supplemental Material [48].

Weak disorder: stable diffusive phase. At weak but non-zero disorder, $0 < W < W_{c1}(\eta)$, the transport is diffusive. This has previously been shown for spin and energy transport in the XXZ chain ($\eta = 0$) [51], but we report it here for the first time in the XYZ case. The diffusive phase is not materially altered when the XY anisotropy is increased, except insofar as it extends to stronger disorder, i.e. $W_{c1}(\eta)$ increases with η (see Fig. 2(b)). We explain in the Supplemental Material how we obtain $W_{c1}(\eta)$ [48].

As in previous studies, we find severe finite-size effects in the results at weak disorder, with the asymptotic scaling behavior of $j^E(L)$ observed only for values of L exceeding a critical length $L^\star$, where $L^\star$ increases with decreasing W. For a ballistic-to-diffusive crossover, it has been shown that this length scale should scale as $L^\star \sim W^{-2}$ [32]. If we apply our analysis naïvely to a chain of length $L < L^\star$, it yields an exponent $\gamma < 1$, and thus falsely suggests superdiffusive energy transport.

However, we can use the scaling properties of $j^E(L)$ to test whether the scaling regime has been reached in any given case. In Fig. 3(a) we demonstrate that, by scaling the data using $x \equiv LW^\nu$ and $y \equiv j^E W^{\delta-\nu}$, it is indeed possible to collapse all points onto a single universal curve. For the example shown, $\eta = 0.4$, the best empirical scaling exponent is $\nu \approx 1.87$, in reasonable agreement with the predicted value of 2. We also find that $\nu - \delta = 0.01$, which is close to the predicted behaviour of $\nu = \delta$ [32].

On the basis of this analysis, we indicate via open symbols in Fig. 2 those cases where the scaling regime has not been reached, and where we are therefore confident that the reported value of γ is not reflective of the thermodynamic limit. Further details of how we identify these points may be found in the Supplemental Material [48].

Intermediate disorder: subdiffusive energy transport. We find that the disordered XYZ model exhibits subdiffusive energy transport at $W > W_{c1}(\eta)$. In contrast to the diffusive region, in the subdiffusive phase the transport exponent γ varies continuously as a function of both the disorder strength W and the XY anisotropy η. This variation shows two main trends. First, as shown in Fig. 2(a), a larger η results in a smaller γ, i.e. breaking the U(1) symmetry pushes the system back towards diffusive transport. Second, as shown in Fig. 2(b), increasing disorder strength W leads to an increased value of γ for all values of η, i.e. increasing disorder pushes the system further away from the diffusive regime. While we cannot follow this behavior all the way to the MBL transition, the location of which we determine by other means, we expect that γ would diverge there.

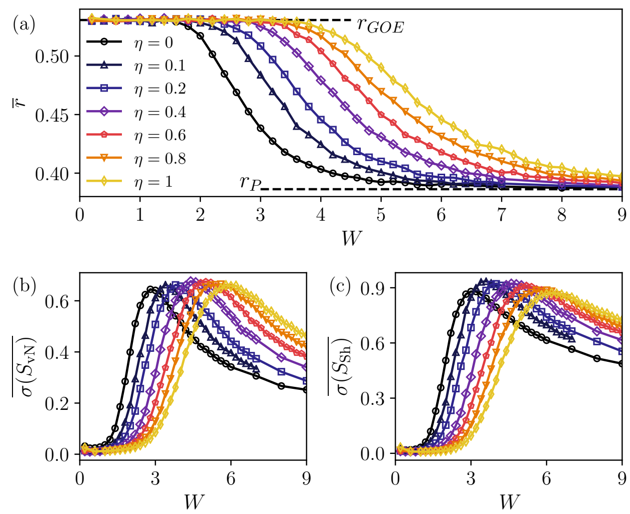

FIG. 4. Locating the MBL transition via exact diagonalization. This figure shows the (a) level statistics r parameter, (b) the standard deviation of the entanglement entropy distribution, and (c) the standard deviation of the Shannon entropy distribution, all as a function of disorder strength W for several values of the XY anisotropy parameter η. These results were obtained from exact diagonalization of the Hamiltonian for a disordered XYZ spin chain of length $L = 15$ with periodic boundary conditions. The error bars are smaller than the symbol size.

Strong disorder: many-body localization. The disorder-averaged level statistics parameter r, and the standard deviations of two types of entropy fluctuation $\sigma(S_{\rm vN})$ and $\sigma(S_{\rm Sh})$, are shown as a function of disorder strength in Fig. 4. All three measures demonstrate a pronounced increase of the critical disorder strength for the MBL transition, W_{c2}, as the XY anisotropy parameter η is increased. The phase diagram in Fig. 1(b) shows the approximate position of the MBL transition according to a scaling analysis of these data. The scaling analysis was performed by numerically collapsing the data for different chain lengths to a function of the form $g(L^{1/\nu}[W - W_{c2}])$, where ν and W_{c2} are fitting parameters, as in previous work [27]. We note that, as found in similar studies, the exponent $\nu < 2$, contrary to established predictions [30].

Discussion. In this paper, we have provided evidence that there are four phases in the disordered spin-1/2 XYZ chain: a ballistic phase at zero disorder; a diffusive phase for a finite range of disorder from 0^+ to a critical value $W_{c1}(\eta)$; a subdiffusive phase for a finite range of disorder from $W_{c1}(\eta)$ to the MBL transition $W_{c2}(\eta)$; and a many-body localized phase for disorders above $W_{c2}(\eta)$. Importantly, the model that we have studied takes us beyond cases — such as the previously studied XXZ chain — that can be thought of in terms of the strongly-interacting dynamics of a fixed number of particles. The XYZ model breaks the U(1) symmetry in a controlled way, and this allows us to observe the changing behavior of the system as we interpolate from the XXZ chain to other models (such as the transverse-field Ising model) which exist in separate regions of parameter space.

The essential physics can be summed up in two short phrases: disorder tends to localize; XY anisotropy tends to delocalize. How should we understand the latter effect? One way is to think in the fermionic picture, in which the XY anisotropy η appears as a pair-creation (and of course a partner pair-annihilation) term. This means that the system, in its time-evolution, can visit sectors with other fermion numbers, which it could not in the XXZ case. Barring significant phase-coherence effects between the states in the N and $N+2$-particle sectors (which there seems to be no reason to expect), this opens up new channels for energy transport, and thus would be expected to enhance the delocalization of energy density excitations. We plan to present further details of this argument in a forthcoming publication [52].

Acknowledgments. We would like to thank Marko Žnidarič, Jonathan Keeling, Roderich Moessner, and Heiko Burau for helpful discussions/comments throughout this project. MS and SRT acknowledge financial support from the CM-CDT under EPSRC (UK) grants EP/G03673X/1 and EP/L015110/1. CAH acknowledges financial support from the TOPNES programme under EPSRC (UK) grant number EP/I031014/1. This research was supported in part by the National Science Foundation under Grant No. NSF PHY-1125915. Part of this work was performed at the Aspen Center for Physics, which is supported by National Science Foundation grant PHY-1066293. AS's research is in part supported by a Google Faculty Award.

[1] S. Will, *From Atom Optics to Quantum Simulation* (Springer-Verlag, 2013).
[2] K. Sattler, ed., *Handbook of Nanophysics: Nanoparticles and Quantum Dots* (CRC Press, 2016).
[3] D. M. Basko, I. L. Aleiner, and B. L. Altshuler, Ann. Phys. **321**, 1126 (2006).
[4] V. Oganesyan and D. A. Huse, Phys. Rev. B **75**, 155111 (2007).
[5] A. Pal and D. A. Huse, Phys. Rev. B **82**, 174411 (2010).
[6] R. Nandkishore and D. A. Huse, Annu. Rev. Condens. Matter Phys. **6**, 15 (2015).
[7] D. A. Abanin and Z. Papić, Ann. Phys. (Berl.) **529** (2017).
[8] P. Anderson, Phys. Rev. **109**, 1492 (1958).
[9] F. Evers and A. D. Mirlin, Rev. Mod. Phys. **80**, 1355 (2008).
[10] N. F. Mott and W. Twose, Adv. Phys. **10**, 107 (1961).
[11] E. Akkermans and G. Montambaux, *Mesoscopic physics of electrons and photons* (Cambridge University Press, 2007).
[12] M. Žnidarič, T. Prosen, and P. Prelovšek, Phys. Rev. B **77**, 064426 (2008).
[13] J. H. Bardarson, F. Pollmann, and J. E. Moore, Phys. Rev. Lett. **109**, 017202 (2012).
[14] M. Serbyn, Z. Papić, and D. A. Abanin, Phys. Rev. Lett. **110**, 260601 (2013).
[15] J. Goold, C. Gogolin, S. R. Clark, J. Eisert, A. Scardicchio, and A. Silva, Phys. Rev. B **92**, 180202 (2015).
[16] F. Iemini, A. Russomanno, D. Rossini, A. Scardicchio, and R. Fazio, Phys. Rev. B **94**, 214206 (2016).
[17] M. Serbyn, Z. Papić, and D. A. Abanin, Phys. Rev. Lett. **111**, 127201 (2013).
[18] D. A. Huse, R. Nandkishore, and V. Oganesyan, Phys. Rev. B **90**, 174202 (2014).
[19] V. Ros, M. Müller, and A. Scardicchio, Nucl. Phys. B **891**, 420 (2015).
[20] J. Z. Imbrie, V. Ros, and A. Scardicchio, Ann. Phys. (Berl.) **529** (2017).
[21] B. Altshuler, H. Krovi, and J. Roland, Proc. Natl. Acad. Sci. U.S.A. **107**, 12446 (2010).
[22] C. Laumann, R. Moessner, A. Scardicchio, and S. Sondhi, Eur. Phys. J. Spec. Top. **224**, 75 (2015).
[23] C. L. Baldwin, C. R. Laumann, A. Pal, and A. Scardicchio, Phys. Rev. Lett. **118**, 127201 (2017).
[24] A. Chandran, A. Pal, C. Laumann, and A. Scardicchio, Phys. Rev. B **94**, 144203 (2016).
[25] W. De Roeck and F. Huveneers, Phys. Rev. B **95**, 155129 (2017).
[26] F. Huveneers, Ann. Phys. (Berl.) **529**, 1600384 (2017).
[27] D. J. Luitz, N. Laflorencie, and F. Alet, Phys. Rev. B **91**, 081103 (2015).
[28] C. R. Laumann, A. Pal, and A. Scardicchio, Phys. Rev. Lett. **113**, 200405 (2014).
[29] W. De Roeck, F. Huveneers, M. Müller, and M. Schiulaz, Phys. Rev. B **93**, 014203 (2016).
[30] A. Chandran, C. R. Laumann, and V. Oganesyan, arXiv: 1509.04285 (2015).
[31] F. Pietracaprina, G. Parisi, A. Mariano, S. Pascazio, and A. Scardicchio, J. Stat. Mech. Theory Exp. **2017**, 113102 (2017).
[32] M. Žnidarič, A. Scardicchio, and V. K. Varma, Phys. Rev. Lett. **117**, 040601 (2016).
[33] Y. Bar Lev, G. Cohen, and D. R. Reichman, Phys. Rev. Lett. **114**, 100601 (2015).
[34] K. Agarwal, S. Gopalakrishnan, M. Knap, M. Müller, and E. Demler, Phys. Rev. Lett. **114**, 160401 (2015).
[35] V. Kerala Varma, A. Lerose, F. Pietracaprina, J. Goold, and A. Scardicchio, J. Stat. Mech. Theory Exp. **2017**, 053101 (2017).
[36] X. Zotos, F. Naef, and P. Prelovsek, Phys. Rev. B **55**, 11029 (1997).
[37] A. V. Savin, G. P. Tsironis, and X. Zotos, Phys. Rev. B **72**, 140402 (2005).
[38] R. Baxter, *Exactly Solved Models in Statistical Mechanics* (London: Academic, 1982).
[39] S. Mukerjee, V. Oganesyan, and D. Huse, Phys. Rev. B **73**, 035113 (2006).

[40] V. Oganesyan, A. Pal, and D. A. Huse, Phys. Rev. B **80**, 115104 (2009).
[41] A. Dymarsky, arXiv: 1804.08626 (2018).
[42] J. Z. Imbrie, J. Stat. Phys. **163**, 998 (2016).
[43] J. A. Kjall, J. H. Bardarson, and F. Pollmann, Phys. Rev. Lett. **113**, 1 (2014).
[44] E. J. Torres-Herrera and L. F. Santos, Ann. Phys. (Berl.) **529**, 1 (2017).
[45] H.-P. Breuer and F. Petruccione, *The Theory of Open Quantum Systems* (Oxford University Press, 2002).
[46] T. Prosen and M. Žnidarič, J. Stat. Mech. Theory Exp. **2009**, P02035 (2009).
[47] M. Žnidarič, T. Prosen, G. Benenti, and D. Rossini, Phys. Rev. E **81**, 051135 (2010).
[48] See Supplemental Material at [URL] for details of numerical simulations, analysis of the disorder-free model, discussion of how we determine W_{c1} and W_{c2}, and the identification of finite-size effects.
[49] J. J. Mendoza-Arenas, S. R. Clark, and D. Jaksch, Phys. Rev. E **91**, 042129 (2015).
[50] J.-S. Caux and J. Mossel, J. Stat. Mech. Theory Exp. **2011**, P02023 (2011).
[51] J. J. Mendoza-Arenas, M. Žnidarič, V. K. Varma, J. Goold, S. R. Clark, and A. Scardicchio, arXiv: 1803.11555 (2018).
[52] M. Schulz, S. R. Taylor, C. A. Hooley, and A. Scardicchio, in preparation (2018).